

## WEAR RATE EVALUATION OF SOL-GEL TiO<sub>2</sub>-ZrO<sub>2</sub> FILMS BY QUANTITATIVE DEPTH PROFILE ANALYSIS

### Summary

Wear resistance of metallic materials can be improved by modifying their surface with different coating deposition techniques, one of which is the sol-gel technology. The sol-gel technology is simple, easy to adopt, requires low processing temperatures and leads to a high degree of purity of oxide coatings. In this paper, the erosive wear resistance of a ceramic nanostructured sol-gel TiO<sub>2</sub>-ZrO<sub>2</sub> film consisting of three layers, deposited on a stainless steel substrate (X5CrNi18-10) by means of the dip coating technique has been studied. Quartz sand was used as an erodent with an impact angle of 30°. Quantitative Depth Profile (QDP) analysis was used for the determination of the coating thickness and chemical composition before and after solid particle erosion. Glow Discharge Optical Emission Spectrometry (GDOES) was used for the analysis of the chemical composition of the bulk material (substrate) and the quantitative depth profiling of the deposited sol-gel film. The obtained results show that solid particle erosion of nanometric films can be monitored by depth profiling of the deposited sol-gel film.

*Key words:* sol-gel, TiO<sub>2</sub>-ZrO<sub>2</sub> film, tribology, quantitative depth profiling

### 1. Introduction

In order to improve the properties of metallic materials, different ceramic coatings may be applied. Ceramic coatings may be deposited on a metallic substrate by numerous and various techniques developed for this purpose. The techniques include physical vapour deposition (PVD), chemical vapour deposition (CVD), electrochemical deposition, thermal spraying, plasma spraying and sol-gel processes, such as spin, dip and spray coating [1, 2].

The sol-gel technology, also known as chemical solution deposition, is a wet chemical technique, a process involving the following steps: hydrolysis and polycondensation, gelation, aging, drying, densification and crystallization. The most important advantages of the sol-gel process are: low equipment costs, low process temperature, good homogeneity of deposited films and use of substances that do not introduce impurities into the final product. This is why the sol-gel technique may be considered as a green technology [3]. The sol-gel film is one of the most important applications of the sol-gel process. Sol-gel dip coating is potentially less expensive than other conventional thin film forming processes [4].

Metal oxide nanostructures have come into focus of intensive research in the past years due to their potential application as catalysts for photodecomposition, semiconductors, in water treatment and so on [5]. Titanium and zirconium oxides are very promising candidates for the future technology of thin layers because of their good mechanical, thermal and chemical properties [6].

Due to their interesting general properties, titanium oxides (or titania, TiO<sub>2</sub>) have been extensively studied in a wide range of fields, including catalysts, photocatalysts, antibacterial agents and self-cleaning nano-paints. The results of these studies may lead to an improvement in the quality of everyday life [7]. Zirconium oxide (or zirconia, ZrO<sub>2</sub>) films are used as thermal barrier coatings, wear resistance coatings, diffusion barriers, oxygen sensors, under-layers for superconducting films and also where high corrosion-resistant properties are required [8].

Composite ZrO<sub>2</sub>-TiO<sub>2</sub> films are also of significant scientific and technological importance, because several advantages can be derived from this binary composite system. The most attractive advantage is that the properties of the composite materials can be tailored by controlling the system. Moreover, the composite material often exhibits better mechanical and thermal properties than the two participating components [9].

In the present study, sol-gel ZrO<sub>2</sub>-TiO<sub>2</sub> three layer films were deposited on a stainless steel X5CrNi18-10 (AISI 304) substrate. The goal of the study was to investigate the effect of the heat treatment, performed on crackles on the sol-gel three layer ZrO<sub>2</sub>-TiO<sub>2</sub> film, on the surface morphology as well as the sand erosion and tribological behaviour of this film.

## 2. Material and methods

### 2.1 Substrate preparation

In this study, two samples (dimensions: 17 × 17 × 80 mm) of stainless steel X5CrNi18-10 (AISI 304) were used as substrates for the sol-gel deposition. The bulk chemical composition of the stainless steel was determined by means of GDOES (GDS 850A, Leco, Czech Republic) and the results are presented in Table 1.

**Table 1** Chemical composition of stainless steel substrate (in terms of weight percentage of the elements)

<i>wt. %</i>									
C	P	S	Si	Mn	Cu	Cr	Ni	Mo	Fe
0.06	0.037	0.006	0.38	1.18	0.32	17.9	7.76	0.16	balance

Prior to the coating deposition, the samples were ground with SiC abrasive discs of different granulation (180-1000 grit) and then polished with diamond paste (3 μm and then 0.25 μm). Thereafter, the substrates were ultrasonically cleaned first in acetone, then in ethanol and finally in the distilled water, each for 10 min and subsequently dried in an oven at 100°C for an hour.

## 2.2 Sol-gel deposition of TiO<sub>2</sub>-ZrO<sub>2</sub> film on the stainless steel substrate

For the preparation of the precursor solution (the so-called sol, or colloidal solution) for the synthesis of the TiO<sub>2</sub>-ZrO<sub>2</sub> film, the following components were used:

- 0.5 mol of titanium isopropoxide and 0.5 mol zirconium butoxide (molar ratio 1:1) as a precursor
- 0.8 mol acetylacetonate as a chelating agent
- 40 mol of i-propanol as a solvent
- 0.05 mol of nitric acid as a catalyst
- 5 mol of distilled water for hydrolysis.

The final precursor sol was yellow, transparent and homogeneous.

The films were deposited on two equal samples of stainless steel. The stainless steel samples were coated by applying the dip coating technique using an in-house developed, electrically driven pulley system. The steel substrates were vertically immersed once into the precursor sol with a constant rate of 10 mm/min, then left to rest in the solution for 3 minutes in order to allow the surface wetting, and finally withdrawn from the sol using the same rate (Figure 1). After each dipping, the samples were air dried for an hour and subsequently dried in an oven at 100°C also for an hour. The whole deposition procedure was repeated three times, in order to increase the coating thickness. Sample 1 (three-layer TiO<sub>2</sub>-ZrO<sub>2</sub> film) was heat treated (calcined) after each dipping and drying procedure, while Sample 2 was calcined only after the third dipping and drying cycle. The calcination was conducted in the following way: the samples were heated to 500°C at a rate of 2°C/min, held at this temperature for an hour and then cooled down by turning the furnace off and keeping it closed.

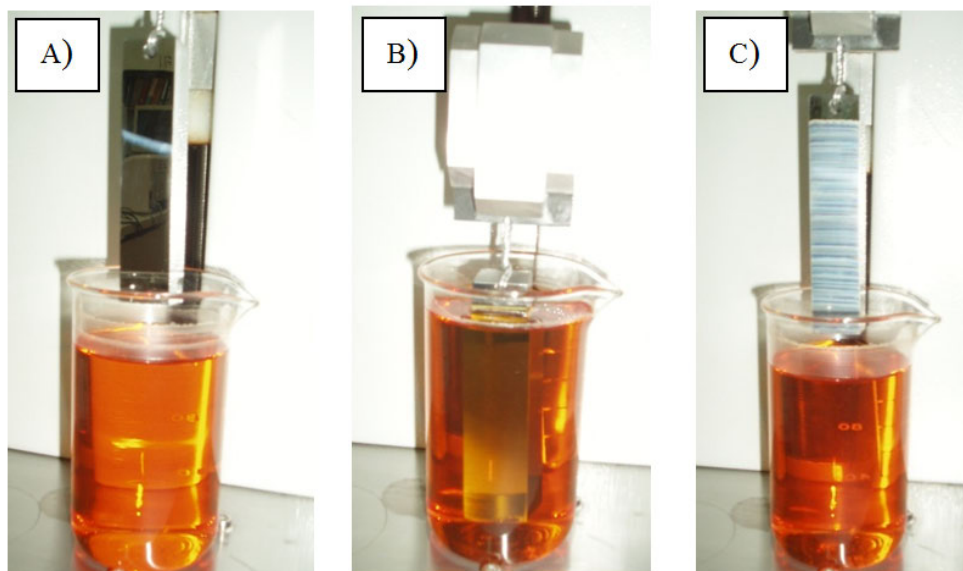


**Fig. 1** Film deposition procedure: (A) dipping; (B) holding; (C) withdrawing.

## 2.3 Characterization of sol-gel TiO<sub>2</sub>-ZrO<sub>2</sub> film

The surface morphological properties of Sample 1 and Sample 2 coated with the sol-gel TiO<sub>2</sub>-ZrO<sub>2</sub> film were examined under the inverted optical microscope (Olympus GX 51, Japan).

Thickness measurement and Quantitative Depth Profile (QDP) analysis of the sol-gel TiO<sub>2</sub>-ZrO<sub>2</sub> films were carried out by means of a glow discharge optical emission spectrometer.

#### 2.4 Solid particle erosion test

Solid particle erosion is a wear mechanism which induces mass loss from the surface of a solid body, and is caused by a relative motion between the body and the fluid containing solid particles. The test of solid particle erosion with quartz sand was performed by means of a particle erosion tester (Figure 2).

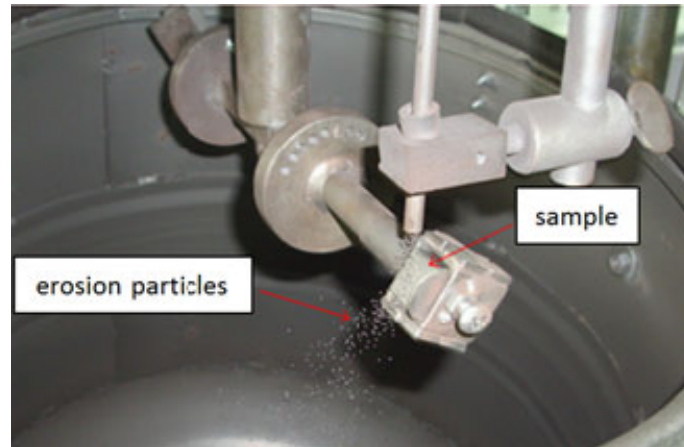


**Fig. 2** Solid particle erosion testing [10].

The testing parameters applied in the solid particle erosion test are:

- Erosion particles: quartz sand (diameter: 212-300  $\mu\text{m}$ )
- Revolution: 1440 rpm
- Sample velocity: 24.3 m/s
- Time of testing: 8.5, 21, 42 s (i.e. 200, 500, 1000 impacts)
- Impact angle: 30°
- Sample dimension: 17  $\times$  17  $\times$  17 mm.

The non-eroded and the eroded samples were subjected to the Quantitative Depth Profiling analysis.

### 3. Results and discussion

Figure 3 shows the surface morphology of TiO<sub>2</sub>-ZrO<sub>2</sub> films (Sample 1 and Sample 2) examined by means of the optical microscope. It is clear that the obtained Sample 1 (TiO<sub>2</sub>-ZrO<sub>2</sub> three layer film, heat treated after the deposition of each layer) was smooth and free from cracks. On the other hand, cracks were observed on the surface of Sample 2 (TiO<sub>2</sub>-ZrO<sub>2</sub> three layer film obtained by applying heat treatment only once after three dipping and drying cycles had been completed). It is assumed that the cracking occurred due to simultaneous calcination of all three layers, i.e. because the coating layer was thicker. Since cracked TiO<sub>2</sub>-ZrO<sub>2</sub> films are unacceptable for usage, further erosion tests were performed only on Sample 1.

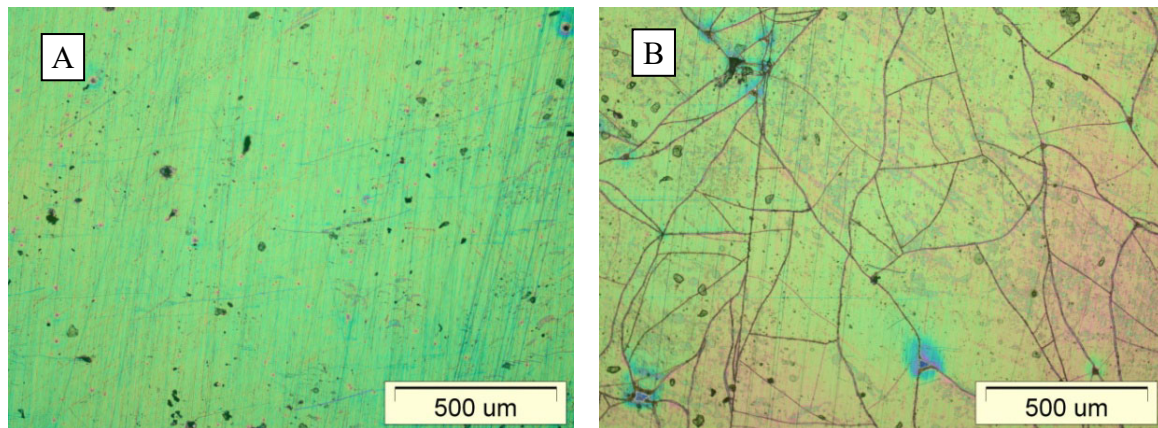


**Fig. 3** Optical microscopy image of deposited sol-gel TiO<sub>2</sub>-ZrO<sub>2</sub> films on stainless steel substrate: (A) Sample 1: TiO<sub>2</sub>-ZrO<sub>2</sub> three layer film heat treated after each layer deposition; (B) Sample 2: TiO<sub>2</sub>-ZrO<sub>2</sub> three layer film obtained by only one heat treatment after three dipping and drying cycles.

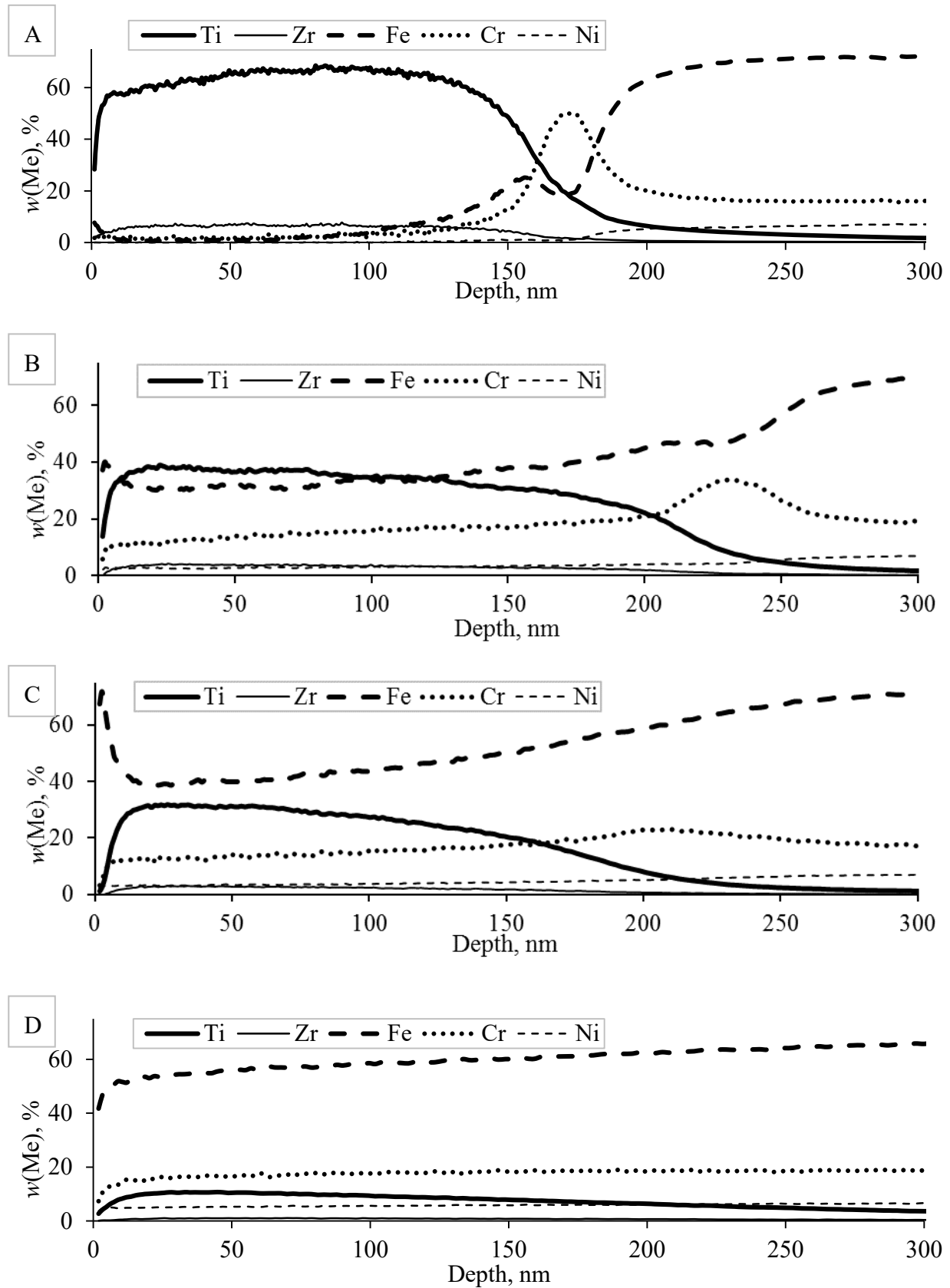
A glow discharge optical emission spectrometer was used for the chemical analysis of both the deposited films and the substrate. This device can be used for elemental bulk analysis, but it can also be used for the determination of the coating thickness and Quantitative Depth Profiling (QDP). In other words, the spectrometer can show the chemical composition of a coating, as well as the distribution of chemical elements from the surface towards the substrate.

The distribution of the most important elements from the surface towards the substrate before and after the erosion test are shown in Figure 4, where  $w(\text{Me})$  is the weight content of the metal (Ti, Zr, Ni, Cr or Fe). Titanium (Ti) and zirconium (Zr) are present in the coating, while Ni, Cr and Fe are present in the substrate. The device that was used is not equipped with an oxygen photomultiplier so the oxygen content was not determined. Possible oxygen content would prove the presence of titanium and zirconium oxide, but not the presence of titanium and zirconium as alloying elements in the substrate material.

It can be seen from Figure 4 (A) that the coating thickness was slightly greater than 150 nm. The diffusion of Fe and Cr from the substrate into the coating was noticed too. It has also been noticed that Cr is significantly diffused from the stainless steel substrate into the interlayer between the steel substrate and the coating, where the formation of chromium oxides might have occurred as well.

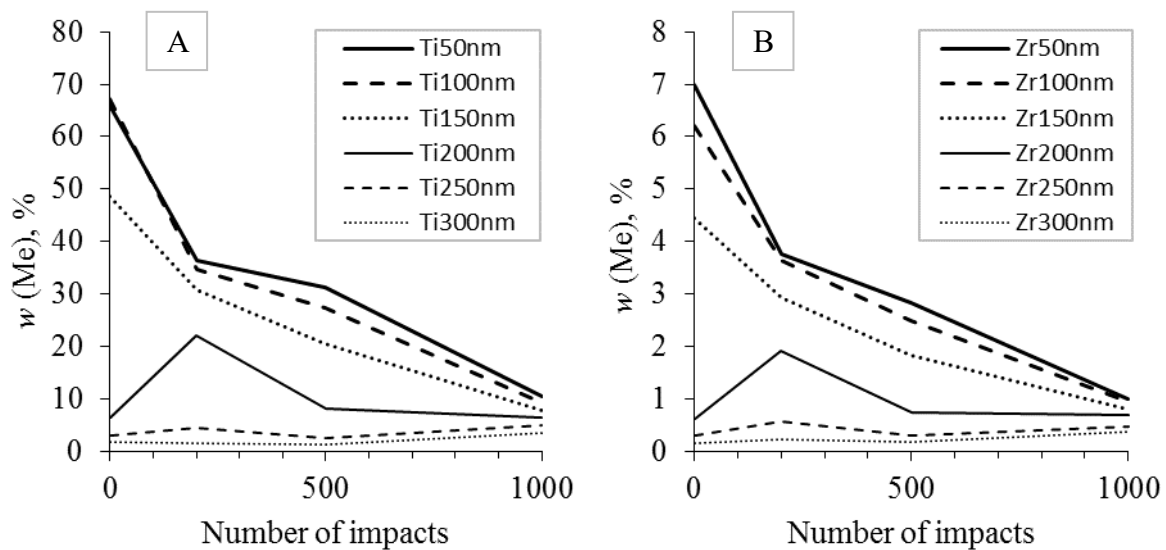
The comparison of Figures 4A and 4B shows a shift in the maximum chromium content to a greater depth after 200 erodent impacts. This means that the chromium oxide interlayer is pressed into the soft steel substrate. With the increase in the number of impacts (Figures 4C and 4D), the chromium oxide interlayer cannot be noticed any more.

Figure 4 shows that as the number of erosive impacts to the surface increases, the content of the chemical elements of the coating decreases, not only on the surface of the sample, but also below the surface at depths less than the thickness of the coating.



**Fig. 4** Quantitative depth profile analysis of sol-gel TiO<sub>2</sub>-ZrO<sub>2</sub> film on stainless steel surface (Sample 1):  
(A) non-eroded; (B) eroded after 200 impacts; (C) eroded after 500 impacts;  
(D) eroded after 1000 impacts.

Figure 5 shows a change in the weight content of titanium and zirconium at different layer depths depending on the number of erosive impacts (e.g. the Ti50nm curve indicates a change in the weight content of titanium at 50 nm from the surface). The same curve shape may be noticed for Ti and Zr. With the number of erosive impacts increasing, the weight content of the coating elements (Ti and Zr) decreases at the expense of the substrate elements. The only deviation is registered after 200 impacts and only at a depth of 200 nm (slightly more than the initial coating thickness). This means that during wear, except for a part of the coating that is removed from the surface, a part of the coating is pressed into the soft steel substrate as well.



**Fig. 5** Decrease in element content in coating at different layer depths due to a different number of erosive impacts: (A) titanium; (B) zirconium.

The actual wear of thin coatings is difficult to determine by measuring only the change in mass (or volume) due to the small weight (or volume) loss during the test. Therefore, this paper proposes a novel model for expressing the amount of wear by monitoring the fluctuation of the content of chemical elements in the coating and substrate. Namely, the partial wear of the coating decreases the content of chemical elements which make up the coating (Ti and Zr) and increases the content of chemical elements normally found in the substrate (Fe, Cr, Ni).

From the obtained results of the QDP analysis, the wear rate of the coating after a certain number of erosive impacts may be estimated. Two different models have been used for calculating the wear rate, depending on whether it is a chemical element from the coating, or a chemical element from the substrate.

The coating wear rate of different chemical elements of the coating may be calculated by using the following equation:

$$\text{Wear rate} = \left( 1 - \frac{w(\text{Me})_a}{w(\text{Me})_b} \right) \times 100, \% \quad (1)$$

where  $w(\text{Me})_a$  is the chemical element (i.e. metal) mass fraction in the coating after the erosion and  $w(\text{Me})_b$  is the element (metal) mass fraction in the coating before the erosion.

The coating wear rate of different chemical elements from the substrate may be calculated by using the following equation:

$$\text{Wear rate} = \frac{w(\text{Me})_a - w(\text{Me})_b}{w(\text{Me})_s - w(\text{Me})_b} \times 100, \% \quad (2)$$

where  $w(\text{Me})_s$  is the element (metal) mass fraction in the substrate,  $w(\text{Me})_a$  is the element (metal) mass fraction in the coating after the erosion and  $w(\text{Me})_b$  is the element (metal) mass fraction in the coating before the erosion.

Since the particle size of the testing abrasive (212-300 μm) is much larger than the coating thickness (~150 nm), the assumptions of the proposed model are that at all testing depths which are lower than the coating thickness the wear rate of all analysed chemical elements would be uniform and that the total wear rate would increase with the number of impacts of the abrasive onto the sample surface. The changes in the content of the chemical elements were analysed at three different coating depths: 50, 100 and 150 nm. The obtained results are shown in Figure 6.

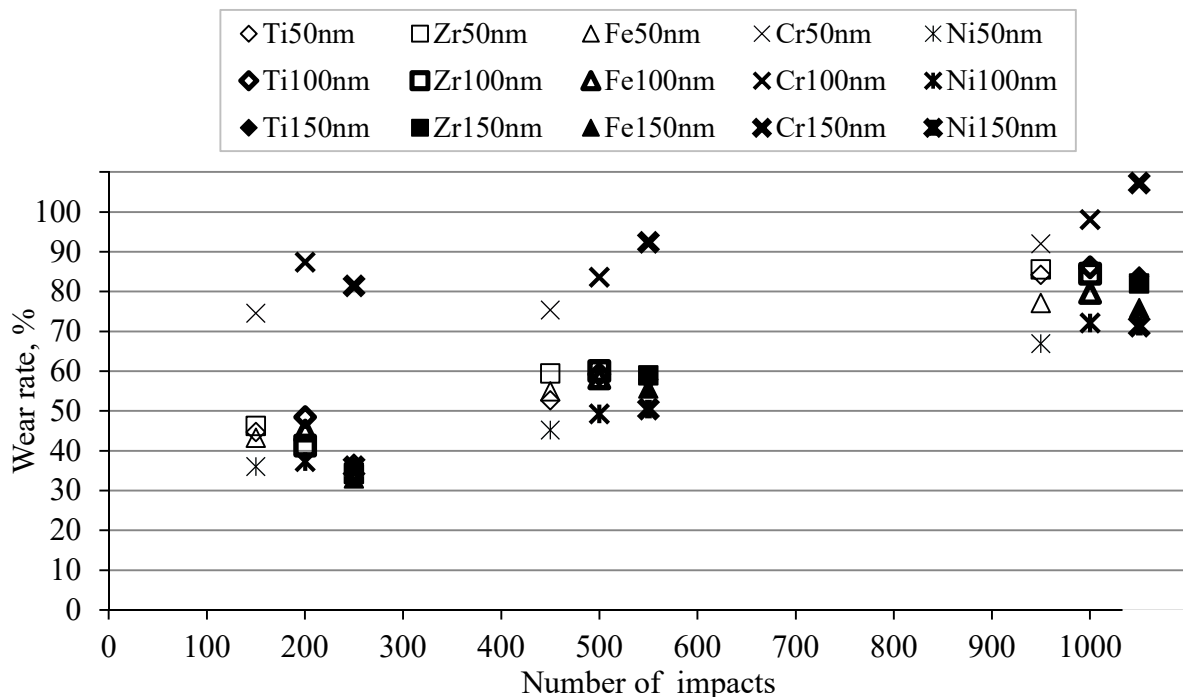
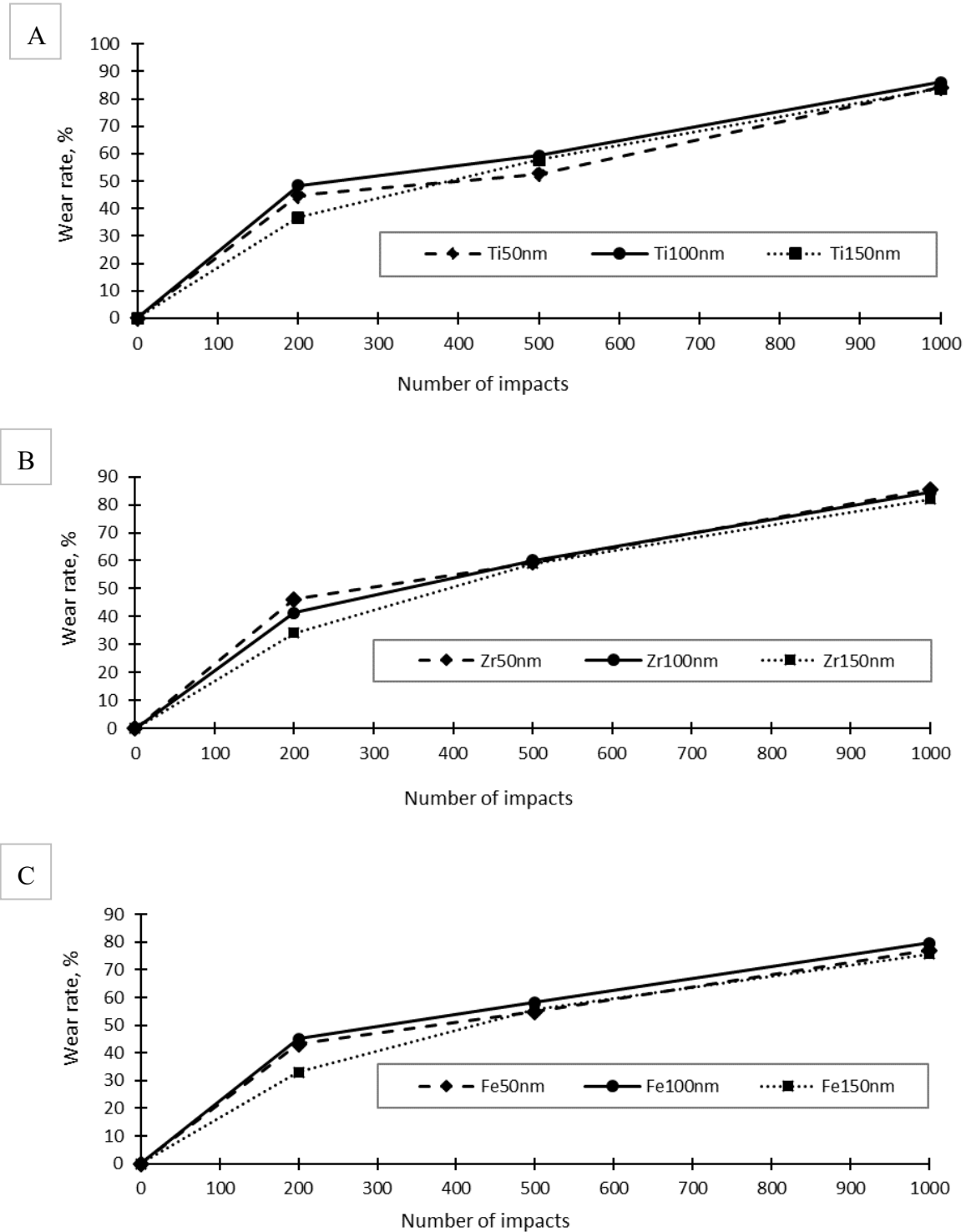


**Fig. 6** Estimated wear rate of titanium and zirconium in the coating and of iron, chromium and nickel in the substrate depending on distance from surface and number of erosive impacts.

Figure 6 shows a significant positive correlation between the wear rate and the number of erosive impacts expressed by the change in the Ti, Zr and Fe content at all three coating depths. A slightly larger variation of the estimated wear rate is indicated by monitoring the Ni content. On the other side, the wear rate results obtained by measuring the chromium content differ significantly. In addition, an unsatisfactory result is obtained for one measuring point (chromium wear rate at 150 nm depth), since the calculated coating wear rate is greater than 100%. The reason for this is that chromium was included in the model as a chemical alloying element of the substrate itself. However, Figure 4A shows that chromium, in addition to being an alloying element in the steel substrate, is also present in the chromium oxide compound in the interlayer formed during the heat treatment of the deposited TiO<sub>2</sub>-ZrO<sub>2</sub> layers.

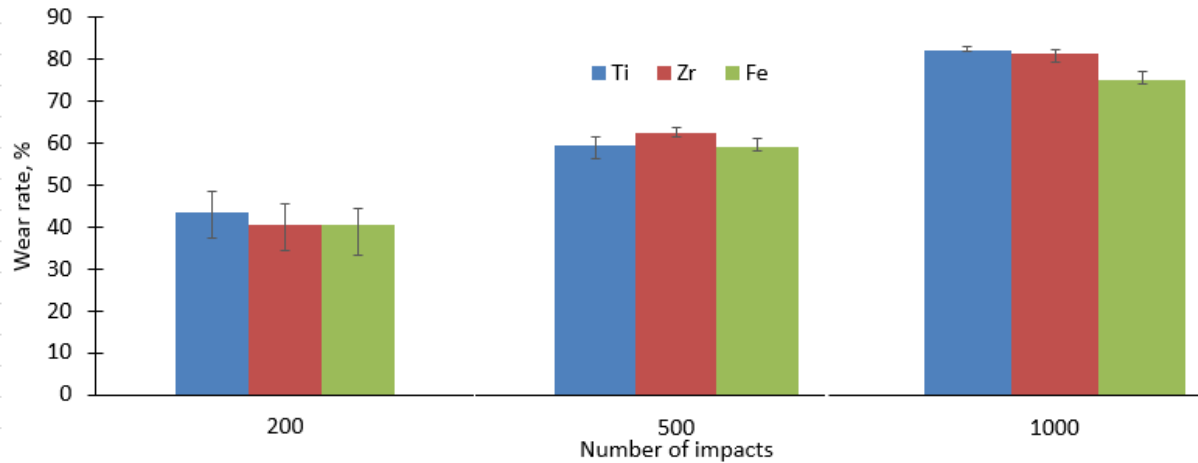


Figure 7 shows the estimated wear rates by monitoring titanium, zirconium and iron depending on the distance from the coating surface. Since the estimated wear rate determined by the monitoring of the chromium and nickel content showed a greater deviation than titanium, zirconium and iron, chromium and nickel were excluded from these additional graphical analyses. In the first part of the test, i.e. up to 200 impacts, a higher estimated wear rate for all the elements was observed. Subsequently, after 200 impacts the course of the estimated wear rate became approximately linearly dependent on the number of impacts.



**Fig. 7** Estimated wear rate depending on distance from surface and number of erosive impacts: (A) titanium; (B) zirconium; (C) iron.

Figure 8 shows mean values of the three estimated wear rates, estimated based on the change in the titanium, zirconium and iron content for different number of impacts (200, 500 and 1000). In addition to the mean value, the data deviations are also shown as error bars for the data at different distances from the surface where the weight content of the individual element was measured, i.e. the maximum and minimum measured values of wear.



**Fig. 8** Mean values and deviations (maximum and minimum values) of wear of individual chemical elements at different distances from sample surface

It can be seen from Figure 8 that the deviations of the estimated wear depending on the distance from the surface of the sample are the greatest in the case of a smaller number of erosive impacts (200) for all three chemical elements: titanium, zirconium and iron. The deviation of the estimated wear data is clearly lower at 500 erosive impacts. Similarly, the wear deviation is further reduced at 1000 impacts. This indicates that the presented wear estimation models are more accurate at higher wear rates.

#### 4. Conclusion

The sol-gel technology and the dip coating technique are confirmed to be convenient techniques for the deposition of the composite TiO<sub>2</sub>-ZrO<sub>2</sub> coating on a stainless steel substrate. The diffusion of elements from the substrate into the coating and vice versa, which occurred during the heat treatment, has been noticed.

During the erosion testing, the coating was partially broken through. After the erosion test, there were lower amounts of titanium and zirconium on the surface, but titanium and zirconium were distributed deeper within the steel substrate, indicating that the coating was partially pressed into the substrate. The reason for this may be higher hardness of the coating compared to the substrate.

It is difficult to determine the wear rate of thin coatings by measuring only the change in mass (or volume) due to the small weight (or volume) loss during the test. Quantitative Depth Profiling (QDP) analysis, i.e. the comparison of the chemical composition of the coatings and the substrate material at different distances from the surface before and after the wear, and the application of the two proposed models for calculating the wear rate may effectively be used for the estimation of wear resistance of very thin coatings.

## REFERENCES

- [1] Dai, W.X.; Chen, X.; Li, E.; Wang, X.X.; Liu, P.; Fu, X.Z. *Influence of pH value of TiO<sub>2</sub> sol on surface gloss of corresponding TiO<sub>2</sub> film coated on ceramic tiles*, Surface Engineering **2009**, 25 (2), 106-109. <https://doi.org/10.1179/174329408X326498>
- [2] Fu, T.; Wen, C.S.; Lu, J.; Zhou, Y.M.; Ma, S.G.; Dong, B.H.; Liu, B.G. *Sol-gel derived TiO<sub>2</sub> coating on plasma nitrated 316L stainless steel*, Vacuum **2012**, 86, 1402-1407. <https://doi.org/10.1016/j.vacuum.2012.01.017>
- [3] Čurković, L.; Otmačić Čurković, H.; Salopek, S.; Majić Renjo, M.; Šegota, S. *Enhancement of corrosion protection of AISI 304 stainless steel by nanostructured sol-gel TiO<sub>2</sub> films*, Corrosion Science **2013**, 77, 176-184. <https://doi.org/10.1016/j.corsci.2013.07.045>
- [4] Vasconcelos, D.C.L.; Nunes, E.H.M.; Sabioni, A.C.S.; Vasconcelos, P.M.P.; Vasconcelos, W.L. *Optical characterization of 316L stainless steel coated with sol-gel titania*, Journal of Non-Crystalline Solids **2012**, 358, 3042-3047. <https://doi.org/10.1016/j.jnoncrysol.2012.07.035>
- [5] Kitiyanan, A.; Sakulkaemaruethai, S.; Suzuki, Y.; Yoshikawa, S. *Structural and photovoltaic properties of binary TiO<sub>2</sub>-ZrO<sub>2</sub> oxides system prepared by sol-gel method*, Composites Science and Technology **2006**, 66, 1259-1265. <https://doi.org/10.1016/j.compscitech.2005.10.035>
- [6] Bensouyad, H.; Sedrati, H.; Dehdouh, H.; Brahimi, M.; Abbas, F.; Akkari, H.; Bensaha, R. *Structural, thermal and optical characterization of TiO<sub>2</sub>:ZrO<sub>2</sub> thin films prepared by sol-gel method*, Thin Solid Films **2010**, 519, 96-100. <https://doi.org/10.1016/j.tsf.2010.07.062>
- [7] Haider, A.J.; Jameel, Z.N.; Al-Hussaini, I.H.M. *Review on: Titanium Dioxide Applications*, Energy Procedia **2019**, 157, 17-29. <https://doi.org/10.1016/j.egypro.2018.11.159>
- [8] Dominguez-Crespo, M.A.; Garcia-Murillo, A.; Torres-Huerta, A.M.; Carrillo-Romo, F.J.; Onofre-Bustamante, E.; Yanez-Zamora, C. *Characterization of ceramic sol-gel coatings as an alternative chemical conversion treatment on commercial carbon steel*, Electrochimica Acta **2009**, 54 (10), 2932-2940. <https://doi.org/10.1016/j.electacta.2008.11.023>
- [9] Liang, L.; Sheng, Y.; Xu, Y.; Wu, D.; Sun, Y. *Optical properties of sol-gel derived ZrO<sub>2</sub> TiO<sub>2</sub> composite films*, Thin Solid Films **2007**, 515 (20-21), 7765-7771. <https://doi.org/10.1016/j.tsf.2007.03.142>
- [10] Jakovljević, S.; Grilec, K. *A study on erosion of ductile cast iron*, Transactions of FAMENA **2009**, 33 (3), 43-50.

Submitted: 09.3.2020

Accepted: 19.7.2020

Krešimir Grilec\*  
Lidija Čurković  
Irena Žmak  
Faculty of Mechanical Engineering and  
Naval Architecture  
Ivana Lučića 5  
10000 Zagreb  
Croatia  
\*kresimir.grilec@fsb.hr